



The impacts of pollution sources and temperature on the light absorption of HULIS were revealed by UHPLC-HRMS/MS at the molecular structure level

Tao Qiu^a, Yanting Qiu^b, Yongyi Yuan^a, Rui Su^c, Xiangxinyue Meng^b, Jialiang Ma^d, Xiaofan Wang^b, Yu Gu^a, Zhijun Wu^{b,*}, Yang Ning^a, Xiuyi Hua^a, Dapeng Liang^{a,*}, Deming Dong^a

^a Key Lab of Groundwater Resources and Environment of the Ministry of Education, College of New Energy and Environment, Jilin University, Changchun 130012, China

^b State Joint Key Laboratory of Environmental Simulation and Pollution Control, College of Environmental Sciences and Engineering, Peking University, Beijing 100871, China

^c State Key Laboratory of Inorganic Synthesis and Preparative Chemistry, College of Chemistry, Jilin University, Changchun 130012, China

^d Department of Chemistry, Aarhus University, 8000 Aarhus C, Denmark

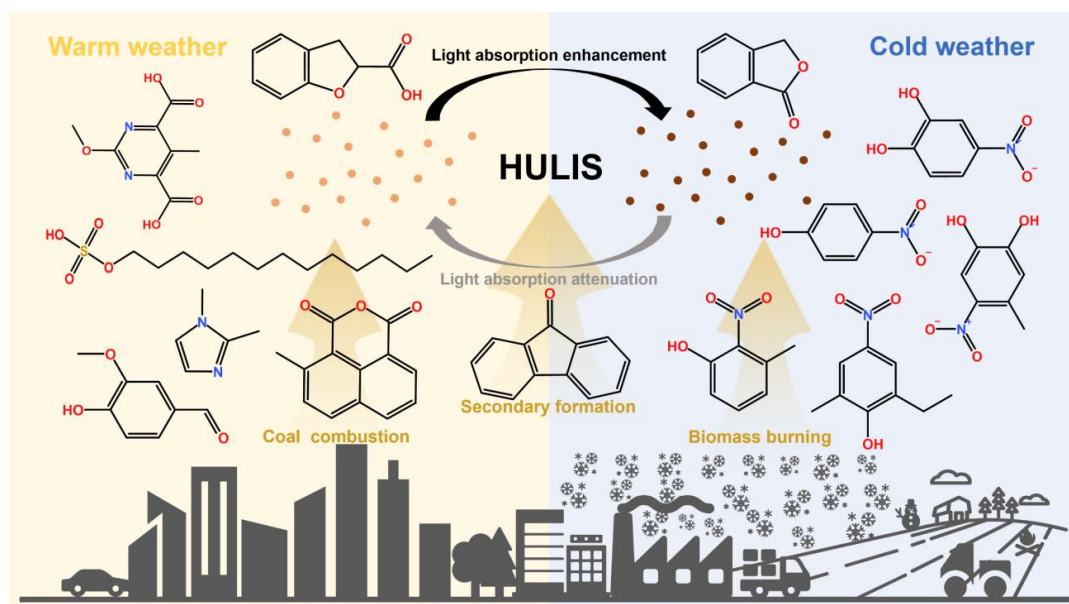
*Corresponding Author: Dapeng Liang (liangdp@jlu.edu.cn) and Zhijun Wu (zhijunwu@pku.edu.cn)

ABSTRACT. Atmospheric humic-like substances (HULIS), a key component of brown carbon (BrC), significantly promote the light absorption of aerosols. However, their linkages to pollution sources and ambient temperature in cold environments remain unresolved. Here, we analyze wintertime urban aerosol samples in Changchun, Northeast China, using ultrahigh performance liquid chromatography coupled with high-resolution tandem mass spectrometry (UHPLC-HRMS/MS). HULIS show a high light absorption efficiency ($MAE_{365} = 1.81 \pm 0.24 \text{ m}^2 \text{ gC}^{-1}$) and high mass concentration ($2.97 \pm 1.54 \mu\text{gC m}^{-3}$), exceeding values reported from other global regions. Through UHPLC-HRMS/MS characterization, we identify 264 compounds at the molecular structure level, accounting for 38.2 - 78.1% of the total HULIS mass. Compositional analysis demonstrates biomass burning and coal combustion are the main BrC sources during haze events. We screen out 39 strong BrC chromophores, mainly nitrophenols, that contribute $28.9 \pm 10.4\%$ of the total light absorbance at 365 nm. Low ambient temperatures potentially enhance the accumulation of these strong BrC chromophores in the aerosol particles by suppressing photobleaching processes and altering thermodynamic reaction equilibria. These findings emphasize the potential of BrC to exert a more significant and persistent environmental effect in the cold region atmosphere.

KEYWORDS: Humic-Like Substances, Non-targeted screening, Northeast China, Light absorption efficiency, Brown carbon chromophores.



29 Graphical Abstract



30



31 1. Introduction

32 Atmospheric humic-like substances (HULIS) are important components in light-absorbing aerosols (Hoffer et al.,
33 2006; Zou et al., 2023), therefore affecting global radiative forcing and atmospheric chemical processes (Chung et al.,
34 2012; Huang et al., 2020; Laskin et al., 2015). They are identified as a highly complex aggregate of polar organic
35 compounds composed of aromatic, aliphatic, and alicyclic structures with functional groups such as hydroxy, carbonyl,
36 carboxyl, nitrooxy, and sulfooxy (Song et al., 2018; Wang et al., 2019; Zou et al., 2023). Previous studies have revealed
37 that the molecular composition of HULIS determine their physicochemical properties, further impacting their climatic
38 and environmental effects, such as cloud condensation nuclei activation, human health, and global radiation (Bao et
39 al., 2023; Cappiello et al., 2003; Chen et al., 2021; Dou et al., 2015; Hems and Abbatt, 2018; Krivácsy et al., 2000).

40 As reactive components in the atmosphere, HULIS exhibit pronounced chemical activity through their
41 oxygenated functional groups, particularly prone to the oxidation by reactive oxygen radicals and gaseous oxidants
42 (Huo et al., 2021; Qiu et al., 2024). Both laboratory simulations and field observations have demonstrated that these
43 aging processes significantly alter the light-absorption features and environmental behavior of HULIS (Hems and
44 Abbatt, 2018; Qiu et al., 2024; Wang et al., 2022, 2019). Although extensive investigations have characterized the
45 elemental composition of HULIS (Lin et al., 2012; Song et al., 2018, 2022a; Wang et al., 2017a, 2019; Zou et al.,
46 2023), critical knowledge gaps persist regarding the molecular structures determining their light absorption. This limits
47 comprehension understanding of the atmospheric evolution process and radiative effect of HULIS.

48 Following emissions into the atmosphere, HULIS undergo vertical transport accompanied by sharp ambient
49 temperature declines (Chen et al., 2021; Slade et al., 2017). This indicates that the atmospheric evolution of HULIS is
50 under low-temperature conditions during their majority lifetime. How low temperature impact the atmospheric
51 evolution process of HULIS remains uncertain yet. The decrease in temperature could potentially alter the
52 physicochemical properties of HULIS, influencing their volatility (Cao et al., 2018; Schervish and Donahue, 2020),
53 reactivity (Liu et al., 2023; Slade et al., 2017), and partitioning between the gas and particulate phase (Arp et al., 2008;
54 Tao and Murphy, 2021). Consequently, their light absorption and atmospheric lifetime might be profoundly affected
55 (Gregson et al., 2023; Roelofs, 2013). Therefore, it is imperative to further explore the low-temperature behavior of
56 HULIS through field observations in cold environments.

57 This study collected atmospheric PM_{2.5} samples in Changchun, which experiences low temperatures in
58 wintertime, and HULIS were subsequently extracted. By employing a combination of non-targeted analysis and
59 ultrahigh performance liquid chromatography coupled with high-resolution tandem mass spectrometry (UHPLC-
60 HRMS/MS), we aimed to identify the molecular structures in HULIS collected from urban aerosols during wintertime.
61 This approach provided us new insights into the potential sources and temperature effects on the light-absorption
62 properties of HULIS.

63 2. Experimental Section

64 **2.1 Aerosol sampling and HULIS extraction.** We conducted a field campaign on the campus of Jilin University
65 in Changchun, Northeast China (125.29° E, 43.83° N) from January 1st to 30th, 2023. During this period, a high-
66 volume particulate sampler (Tianhong Intelligent Instrument Plant, Wuhan, China, 1.05 m³ min⁻¹) collected 24 h PM_{2.5}



67 samples on a pre-baked quartz filter. **Figure S5** presented the meteorological data (<http://www.wunderground.com/>)
 68 and air pollutants data (<http://air.cnemc.cn:18007/>), including relative humidity, temperature, concentrations of CO,
 69 SO₂, O₃, NO₂, PM_{2.5}, and PM₁₀ during the sampling campaign.

70 The preparation process of HULIS sample was identical with previous studies (Limbeck et al., 2005; Yuan et al.,
 71 2021; Zou et al., 2020), and can be briefly described as the following steps: sampled filter was firstly extracted with
 72 ultrapure water (> 18.2 MΩ) in an ultrasonic bath for 40 mins. After that, the water extracts were filtered through 0.22
 73 μm PES syringe filters, then acidified to pH=2 by HCl solution (0.1 M) and loaded on the pre-acidification solid phase
 74 extraction (SPE) cartridges (Supelclean ENVI-18, 500 mg, 3 mL). The majority of inorganic ions, low molecular-
 75 weight organic acids, and sugars were eluted out with ultrapure water while the fractions retained in the SPE cartridge
 76 were eluted with methanol (Baduel et al., 2009). Finally, a portion of the elution was measured by UHPLC-HRMS/MS
 77 and the rest was dried under a gentle stream of N₂, then redissolved in ultrapure water for total organic carbon and
 78 light absorption analysis.

79 **2.2 Molecular composition analysis of HULIS.** An ultrahigh performance liquid chromatography system
 80 (UHPLC, Dionex Ultimate 3000, Thermo Fisher Scientific, San Jose, CA, U.S.A.) coupled with an Orbitrap Fusion
 81 Tribrid mass spectrometer (Thermo Fisher Scientific, San Jose, CA, U.S.A.) was used to detect the molecular
 82 composition of HULIS. To detect as many HULIS species as possible and achieve quantification, we optimized the
 83 detection method to decrease the method detection limit and applied a semi-quantitative strategy to quantify the
 84 identified compounds (detailed in **Text S1**).

85 The optimized chromatographic conditions were as follows: Accucore C18 2.6 μm particle size (100 × 2.1 mm,
 86 Thermo Scientific) with the gradient elution started from 80% of mobile phase A (0.05% acetic acid) with a 0.2 mL
 87 min⁻¹ flow rate for 2 min, then changed to 100% of mobile phase B (methanol with 0.05% acetic acid) in 15 min and
 88 maintained constant for 2 min, decreased to 20% of mobile phase B within 1 min and finally held for 3 min for re-
 89 equilibration. The mass spectra (*m/z* 60-600) with a resolving power of 120,000 (*m/z* 200) were obtained by using
 90 heated-electrospray ionization (H-ESI). The optimized mass spectrometric parameters were as follows: 3.5 kV spray
 91 voltage for positive ions and 3.25 kV spray voltage for negative ions, 35 psi sheath gas (nitrogen), and 10 psi auxiliary
 92 gas (nitrogen), 320 °C ion transfer tube temperature, 125 °C vaporizer temperature. The data acquisition used data
 93 dependent mode and the master scans interval time was set as 1.0 second for the full scan experiments (detailed in
 94 **Table S4**).

95 **2.3 Light absorption analysis of HULIS and other analysis.** A total of the HULIS extract was first diluted to
 96 3 mL with ultrapure water and then measured by a UV-Vis spectrophotometer (UV-1900, Shimadzu, Kyoto, Japan) at
 97 200-700 nm with an interval wavelength of 1 nm. To assess the optical properties of HULIS samples, the mass
 98 absorption efficiency (MAE_{λ} , m² gC⁻¹) was calculated according to the following formula.

$$99 \quad Abs_{\lambda} = (A_{\lambda} - A_{700}) \frac{V_l}{V_a \times l} \ln 10 \quad (1)$$

$$100 \quad MAE_{\lambda} = \frac{Abs_{\lambda}}{c} \quad (2)$$

101 where Abs_{λ} represents the light absorption coefficient of the HULIS extract at a wavelength of λ nm (Mm⁻¹), A_{λ} is
 102 the recorded absorbance value of the HULIS extract by the UV-Vis spectrophotometer, V_l is the total solution volume



103 of HULIS extract (mL), V_a is the air sampling volume corresponding to the volume of HULIS extract (m^3), l
104 represents the optical path length (0.01 m), C is the mass concentration of HULIS carbon (HULIS-C) ($\mu\text{gC m}^{-3}$).

105 The contents of elemental carbon (EC) and organic carbon (OC) in quartz fiber filters were determined by a
106 Thermo-Optical Transmission (TOT) method on a Sunset Lab EC/OC analyzer. The concentrations of HULIS-C were
107 analyzed by a total organic carbon analysis (TOC-L, Shimadzu, Kyoto, Japan). The water-soluble inorganic ions in
108 $\text{PM}_{2.5}$ collected on Teflon filter were detected by ion chromatography (IC, Shimadzu, Kyoto, Japan). The aerosol liquid
109 water content (ALWC) and pH were calculated using the ISORROPIA II thermodynamic model based on
110 meteorological data and mass concentrations of water-soluble inorganic ions (Fountoukis and Nenes, 2007; Nenes et
111 al., 1998; Wu et al., 2018).

112 3. Results and Discussion

113 **3.1 Molecular composition and light absorption of HULIS.** Figure 1A illustrated the temporal variations of
114 HULIS-C, OC, and EC mass concentrations over the entire sampling period during which temperatures ranged from
115 2.9 to -25.3°C and solar radiation ranged from 24.3 to 57.8 W m^{-2} (Figure 1B). The average concentrations of OC
116 and EC were 11.7 ± 5.74 and $2.06 \pm 0.92 \mu\text{g m}^{-3}$, respectively. The average HULIS-C concentration amounted to 2.97
117 $\pm 1.54 \mu\text{g m}^{-3}$, constituting 25.1% of the total OC. The observed HULIS-C concentration exceeded levels documented
118 in winter of Europe ($0.68 - 1.47 \mu\text{g m}^{-3}$) (Emmenegger et al., 2007; Voliotis et al., 2017), South America ($0.68 - 1.47$
119 $\mu\text{g m}^{-3}$) (Serafeim et al., 2023), Chinese other regions ($1.96 - 2.38 \mu\text{g m}^{-3}$) (Lu et al., 2019; Ma et al., 2019; Zou et
120 al., 2023), indicating the abundance of HULIS in Changchun.

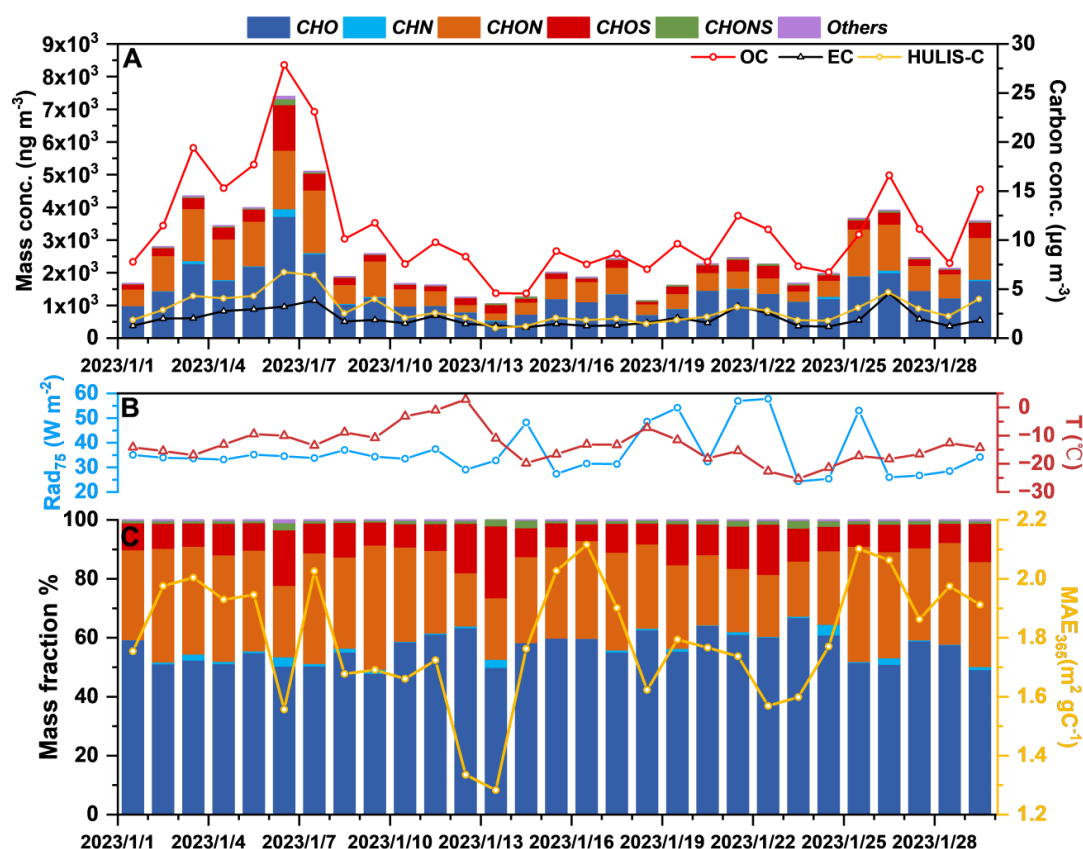


Figure 1. Temporal variations in the mass concentrations of six compound categories, organic carbon, and elemental carbon (A); the 75th percentile of solar radiation (Rad₇₅) and ambient temperature (B); the mass fraction of six compound categories as well as MAE₃₆₅ (C).

Molecular composition analysis of HULIS identified 264 compounds at the molecular structure level. **Table S6** in the supplement listed the details of these HULIS compounds and their corresponding confidence levels. The identified compounds were grouped into six compound categories based on their elemental types, including CHO, CHN, CHON, CHOS, CHONS, and other species. CHONS category refers to compounds that contain carbon, hydrogen, oxygen, nitrogen, and sulfur elements. **Figure 1A and 1C** showed variations of six compound categories. The total mass concentration of these compounds ranged from 1.05 to 7.39 μg m⁻³ (**Figure 1A**), explaining 38.2% - 78.1% of the total HULIS mass (converted by multiplying [HULIS-C] by 1.6, (Friman et al., 2023)). The remaining unidentified compounds in HULIS mainly include low-polarity phenols, ketones, and aldehydes, whose polarity is too low to be ionized in the ESI mode (Huang et al., 2025; Huo et al., 2021; Song et al., 2022b, 2024).

Figure 1C also displayed that MAE at 365 nm (MAE₃₆₅) of HULIS samples. The MAE₃₆₅ ranged from 1.28 to 2.12 m² gC⁻¹ (1.81 ± 0.24 m² gC⁻¹ in average), which was higher than those in Beijing (1.79 ± 0.24 m² gC⁻¹) (Cheng et al., 2011), Xi'an (1.65 ± 0.36 m² gC⁻¹) (Huang et al., 2018), Guangzhou (1.1 ± 0.27 m² gC⁻¹) (Zou et al., 2023), and Hong Kong (0.97 ± 0.40 m² gC⁻¹) (Ma et al., 2019) during wintertime. This indicated that HULIS in Changchun have



higher light absorption efficiency compared to other regions in China. Moreover, the strongly positive correlation (Figure S6) between MAE₃₆₅ with CHON category (Pearson's $R = 0.77$, p -value < 0.01) and aromatic fraction (Pearson's $R = 0.86$, p -value < 0.01) suggested that the high light absorption efficiency of HULIS may be related to aromatic CHON compounds.

3.2 Potential sources of HULIS based on molecular analysis. To analyze the cause of the high concentrations and light absorption efficiency of HULIS in this study, we selected two typical haze events with significant differences in MAE₃₆₅ (Event I: $PM_{2.5} = 159.6 \pm 53.8 \mu g m^{-3}$, $MAE_{365,HULIS} = 1.56 m^2 gC^{-1}$; Even II: $PM_{2.5} = 83.7 \pm 36.4 \mu g m^{-3}$, $MAE_{365,HULIS} = 2.06 m^2 gC^{-1}$) for potential sources comparison from the perspective of molecular composition. Figure 2 exhibited the reconstructed MS spectra, the number, and concentration fraction of HULIS in both positive and negative modes.

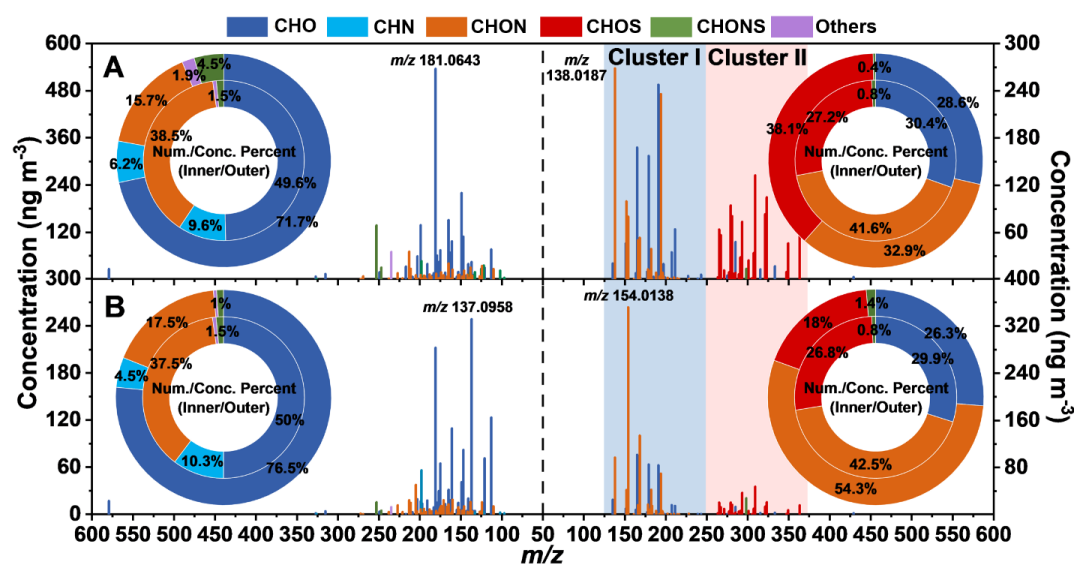


Figure 2. Reconstructed mass spectra (positive ions on the left, while negative ions on the right) for the identified HULIS samples during Event I (A) and Event II (B). The highest peaks were marked by their m/z . The inner and outer ring pie charts were the fraction of mass concentration and numbers in the different categories of the identified compounds, respectively.

In the positive mode, Event I and II had similar elemental composition, both dominated by CHO compounds, followed by CHON, CHN, and others. The most abundant species in Event I and II were 9-fluorenone (m/z 181.0643) and 2-[(1E)-1-Buten-1-yl]-5-methylfuran (m/z 137.0958), respectively. The former originates from diverse combustion sources such as biomass burning, coal combustion, and vehicle emission (Alves et al., 2016; Huo et al., 2021; Ma et al., 2023; Souza et al., 2014; Xu et al., 2024; Zhao et al., 2020), whereas the latter is believed to stem specifically from biomass burning (Bhattu et al., 2019; Hatch et al., 2015). Further evidence for the significant role of biomass burning and coal combustion in both events was provided by the high concentrations of biomass burning tracers (i.e. vanillin, syringaldehyde, acetosyringone in Table S6, and K^+ in Table S5) and SO_2 (Table S5) (Chen et al., 2017; Dutton et al., 2009; He et al., 2010; Liang et al., 2021). Biomass burning and coal combustion have been confirmed in our previous study to be the main sources of air pollution in Changchun winter (Dong et al., 2023).



162 In the negative mode, two distinct compound clusters were observed within the m/z range of 125 – 250 (refer to
163 Cluster I) and 250 – 375 (refer to Cluster II), as marked in the right part of **Figure 2**. Cluster I comprised a significant
164 proportion of strong BrC species, such as nitrophenols (including 4-nitrophenol, 3-nitrocatechol, 4-nitro-1-naphthol,
165 and etc., **Table S6**), mainly originating from primary emissions like biomass burning and coal combustion (Huang et
166 al., 2023; Jiang et al., 2023; Lin et al., 2017; Wang et al., 2020). Notably, Cluster I fraction was more prominent in
167 Event II than Event I, explaining the higher MAE₃₆₅ in the former.

168 All of CHOS compounds were characterized by ion fragment m/z 96.9595 in the MS/MS spectra and were
169 therefore identified as organosulfates (OSs). Considering the OSs are typically formed by atmospheric aqueous
170 reaction (Brüggemann et al., 2017; Pratt et al., 2013; Wach et al., 2020), we therefore proposed that Cluster II which
171 was mainly composed of OSs originated from secondary formation. The higher abundance of Cluster II in Event I
172 suggested that the secondary formation of HULIS was more intense during this event compared to Event II. The
173 elevated concentrations of secondary inorganic ions (including NH_4^+ , NO_3^- , and SO_4^{2-} , 11.35 – 27.66 vs 4.49 – 7.61
174 $\mu\text{g m}^{-3}$) and relative humidity ($83.1 \pm 4.6\%$ vs $61.9 \pm 14.0\%$) in Event I than those in Event II were observed, as
175 detailed in **Table S5**. As a result, the higher ALWC (95.9 vs $23.9 \mu\text{g m}^{-3}$) and lower pH value (4.20 vs 4.82) in Event
176 I in contrast to Event II facilitated the formation of OSs. Since the OSs studied here were primarily aliphatic sulfates
177 (summarized as the molecular formulas of $\text{C}_n\text{H}_{2n+2}\text{O}_{4-6}\text{S}$ and $\text{C}_n\text{H}_{2n}\text{O}_{4-6}\text{S}$, where $10 \leq n \leq 18$), which belong to non-
178 light-absorbing organic matter, this may cause the lower MAE₃₆₅ value in Event I.

179 **3.3 Effect of ambient temperature on the BrC chromophores of HULIS.** As above-mentioned, the
180 temperature was down to -25°C . Such low temperature may affect the evolution of HULIS in the atmosphere. In total,
181 39 compounds were screened as strong BrC chromophores to analyze the effect of temperature on the BrC
182 chromophores according to a partial least squares regression (PLS) model (detailed in **Text S4**). These compounds
183 belong to nitrophenols or nitrophenol derivatives, which are marked in **Table S6**. The 39 strong BrC chromophores
184 accounted for $8.67 \pm 3.68\%$ of the total mass and contributed $28.9 \pm 10.4\%$ of the light absorbance (**Figure S7**), with
185 an average MAE₃₆₅ of $7.40 \pm 1.80 \text{ m}^2 \text{ gC}^{-1}$, indicating their importance in the light absorption of HULIS.

186 **Figure 3** presented that the mass fraction of screened 39 BrC chromophores, along with the MAE₃₆₅ value of
187 HULIS, across different temperature ranges. Both mass fraction and MAE₃₆₅ increased with decreasing ambient
188 temperature, indicating that low temperature may facilitate the accumulation of strong BrC species in the particle
189 phase. We proposed two possible explanations: firstly, the low temperature may lead to a non-liquid phase state of
190 ambient particles, potentially introducing kinetic limitation on the diffusion of reactive species from gas phase into
191 particle bulk (Li and Shiraiwa, 2019). We utilized an established parameterization scheme (**Text S3**) to calculate the
192 glass transition temperature (T_g) of HULIS based on their molecular composition (Li et al., 2020). The results showed
193 that the decrease in ambient temperature (T) enhanced the T_g/T ratio, driving the phase transition of particles from
194 liquid state ($T_g/T = 0.76$) to semi-solid state ($T_g/T > 0.79$). This may lead to the diffusion coefficients reduction of
195 reactive species (Arangio et al., 2015; Gatzsche et al., 2017; Mikhailov et al., 2009; Shiraiwa et al., 2011; Virtanen et
196 al., 2010), thereby slowing the degradation rate of BrC via hydroxyl radical oxidation or triplet excitation pathways
197 in the atmosphere (Schnitzler et al., 2022; Schnitzler and Abbatt, 2018). These findings suggest that the non-liquid
198 particle phase state, in conjunction with the weak solar radiation during Changchun's winter (refer to **Figure 1B**),
199 results in a less pronounced photochemical aging of BrC, thereby diminishing its photobleaching.

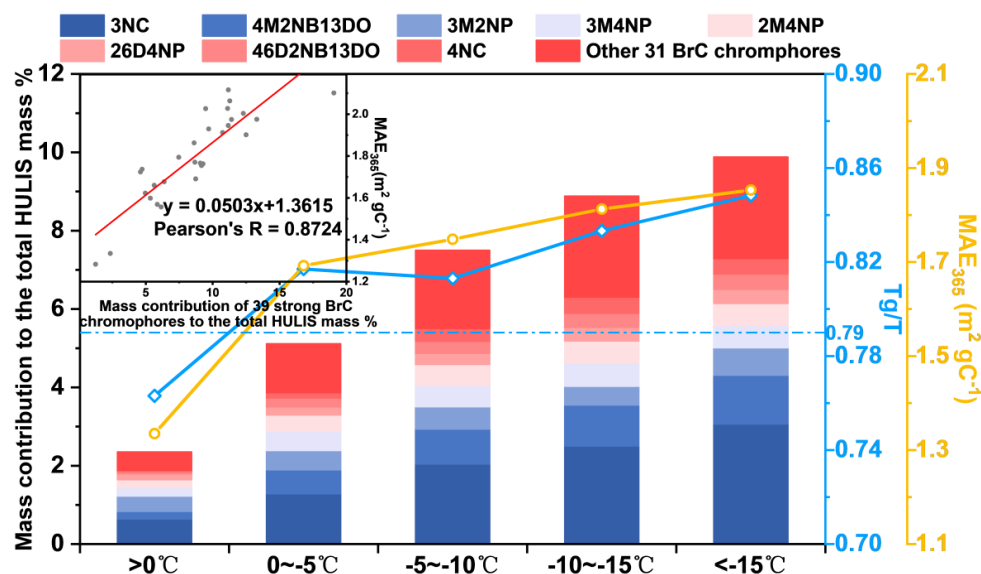


Figure 3. The mass contribution of 39 strong BrC chromophores, MAE_{365} values, ratios of glass transition temperature (T_g) to temperature (T) at different temperatures, and linear relationships between mass contribution of strong BrC and MAE_{365} of HULIS. The blue dotted line represented the threshold of T_g/T between liquid and semi-solid state (Shiraiwa et al., 2017), and the abbreviations of 3NC, 4M2NB13DO, 3M2NP, 3M4NP, 2M4NP, 26D4NP, 46D2NB13DO, and 4NC represents 3-nitrocatechol, 4-methyl-2-nitrobenzene-1,3-diol, 3-methyl-2-nitrophenol, 3-methyl-4-nitrophenol, 2-methyl-4-nitrophenol, 2,6-dimethyl-4-nitrophenol, 4,6-dimethyl-2-nitrobenzene-1,3-diol, and 4-nitrocatechol, respectively.

Secondly, the formation of BrC chromophores was also important for the MAE_{365} enhancement of HULIS. On the one hand, the secondary formation of nitrophenols has been conclusively attributed to reaction of phenols with NO_x radicals (Bolzacchini et al., 2001; Finewax et al., 2018; Kroflič et al., 2021; Mayorga et al., 2021), a process that has been characterized as exothermic (Bolzacchini et al., 2001; Domingo et al., 2021). On the other hand, we have demonstrated that further atmospheric oxidation of nitrophenols proceeds via a ring-opening mechanism of benzene moiety (Qiu et al., 2024), which constitutes an endothermic reaction (Cao et al., 2021; Hems and Abbatt, 2018; Wang et al., 2017b). From a thermodynamic perspective, low temperature not only promotes exothermic chemical reactions but also hinders endothermic processes, thereby accumulating the strong BrC chromophores such as nitrophenols in HULIS. As such, we infer that ambient temperature play a critical role in promoting the transformation and light absorption of BrC chromophores, particularly in cold or/and high-altitude regions.

3.4 Conclusions. In this work, we explored the linkage between the light absorption and molecular structure of atmospheric HULIS in Changchun winter based on UHPLC-HRMS/MS. In different haze events, the molecular structure of HULIS varied due to different sources, which lead to differences in their light absorption efficiency. Biomass burning and coal combustion were important inducers of the high MAE_{365} value of HULIS. It was the fact that biomass burning and coal combustion emitted a large fraction of BrC chromophores such as nitrophenols, while aliphatic organosulfates produced by secondary formation lead to the reduction in the light absorption efficiency of HULIS.

In addition, our study screened out 39 strong BrC chromophores belonging to nitrophenols by PLS model. These



species accounted for $8.67 \pm 3.68\%$ of the total HULIS mass while contributed nearly 30% of the light absorbance at 365 nm. We found that low temperature can promote the accumulation of strong BrC chromophores through slowing down the photobleaching reaction and changing the thermodynamic reaction equilibrium, thereby improving the light absorption capability of HULIS. This phenomenon has not been studied before, and further laboratory and field studies are urgently needed to verify the effect of temperature on the light absorption properties of BrC.

Our research has found that in the cold regions of northern China, on one hand, primary emissions from biomass burning and coal combustion are relatively strong, and on the other hand, low temperatures reduce the photobleaching of brown carbon (BrC). This implies that BrC in cold regions may have a longer lifetime and stronger light-absorbing properties in the atmosphere, thus playing a more significant role in the direct radiative forcing of carbonaceous aerosols.

Supplementary Information. Optimization details of LC-MS method, calculation procedure of relevant index, screening details of PLS model, and analysis results of pollutant data and meteorological data (PDF).

The information about atmospheric mass concentration, molecular information, and strong brown carbon chromophores of identified compounds in HULIS samples of Changchun during wintertime (Table S6).

Author Contributions. T. Q. and Y. Q. designed this work. T. Q., X. W., and Y. G., collected the experimental samples. T. Q., Y. Q., Y. Y., R. S., Y. N., X. H., and X. M. collected and analyzed the experimental data. Z. W., D. L., D. D., and H. C. edited the manuscript. All authors have read and agreed to the published version of the manuscript.

Funding. This work was supported by the National Natural Science Foundation of China (No. 22376084) and Environmental Protection Research Program from Jilin Department of Ecology and Environment (No. 2023-09).

Notes. The authors declare no competing financial interest.

Acknowledgments. Authors of this article wish to thank the financial support from the National Natural Science Foundation of China (No. 22376084) and Environmental Protection Research Program from Jilin Department of Ecology and Environment (No. 2023-09), the technical support from Ms. Huimin Qian and the work support from Mr. Shengao Yang. This work was also supported by State key Laboratory of Inorganic Synthesis and Preparation Chemistry, Jilin University.



250 Reference

- 251 Alves, C. A., Vicente, A. M. P., Gomes, J., Nunes, T., Duarte, M., and Bandowe, B. A. M.: Polycyclic aromatic
252 hydrocarbons (PAHs) and their derivatives (oxygenated-PAHs, nitrated-PAHs and azaarenes) in size-fractionated
253 particles emitted in an urban road tunnel, *Atmos Res*, 180, 128–137,
254 <https://doi.org/10.1016/J.ATMOSRES.2016.05.013>, 2016.
- 255 Arangio, A. M., Slade, J. H., Berkemeier, T., Pöschl, U., Knopf, D. A., and Shiraiwa, M.: Multiphase chemical
256 kinetics of OH radical uptake by molecular organic markers of biomass burning aerosols: Humidity and
257 temperature dependence, surface reaction, and bulk diffusion, *Journal of Physical Chemistry A*, 119, 4533–4544,
258 <https://doi.org/10.1021/JP510489Z>, 2015.
- 259 Arp, H. P. H., Schwarzenbach, R. P., and Goss, K. U.: Ambient gas/particle partitioning. 2: The influence of
260 particle source and temperature on sorption to dry terrestrial aerosols, *Environ Sci Technol*, 42, 5951–5957,
261 <https://doi.org/10.1021/ES703096P>, 2008.
- 262 Baduel, C., Voisin, D., and Jaffrezo, J. L.: Comparison of analytical methods for humic Like Substances (HULIS)
263 measurements in atmospheric particles, *Atmos Chem Phys*, 9, 5949–5962, [https://doi.org/10.5194/ACP-9-5949-](https://doi.org/10.5194/ACP-9-5949-2009)
264 2009, 2009.
- 265 Bao, M., Zhang, Y. L., Cao, F., Hong, Y., Lin, Y. C., Yu, M., Jiang, H., Cheng, Z., Xu, R., and Yang, X.: Impact
266 of fossil and non-fossil fuel sources on the molecular compositions of water-soluble humic-like substances in
267 PM_{2.5} at a suburban site of Yangtze River Delta, China, *Atmos Chem Phys*, 23, 8305–8324,
268 <https://doi.org/10.5194/ACP-23-8305-2023>, 2023.
- 269 Bhattu, D., Zotter, P., Zhou, J., Stefanelli, G., Klein, F., Bertrand, A., Temime-Roussel, B., Marchand, N., Slowik,
270 J. G., Baltensperger, U., Prevot, A. S. H., Nussbaumer, T., Haddad, I. El, and Dommen, J.: Effect of Stove
271 Technology and Combustion Conditions on Gas and Particulate Emissions from Residential Biomass
272 Combustion, *Environ Sci Technol*, 53, 2209–2219, <https://doi.org/10.1021/ACS.EST.8B05020>, 2019.
- 273 Bolzacchini, E., Bruschi, M., Hjorth, J., Meinardi, S., Orlandi, M., Rindone, B., and Rosenbohm, E.: Gas-phase
274 reaction of phenol with NO₃, *Environ Sci Technol*, 35, 1791–1797, <https://doi.org/10.1021/ES001290M>, 2001.
- 275 Brüggemann, M., Poulain, L., Held, A., Stelzer, T., Zuth, C., Richters, S., Mutzel, A., Van Pinxteren, D., Iinuma,
276 Y., Katkevica, S., Rabe, R., Herrmann, H., and Hoffmann, T.: Real-time detection of highly oxidized
277 organosulfates and BSOA marker compounds during the F-BEACH 2014 field study, *Atmos Chem Phys*, 17,
278 1453–1469, <https://doi.org/10.5194/ACP-17-1453-2017>, 2017.
- 279 Cao, L. M., Huang, X. F., Li, Y. Y., Hu, M., and He, L. Y.: Volatility measurement of atmospheric submicron
280 aerosols in an urban atmosphere in southern China, *Atmos Chem Phys*, 18, 1729–1743,
281 <https://doi.org/10.5194/ACP-18-1729-2018>, 2018.
- 282 Cao, T. ting, Xu, T. fu, Deng, F. xia, Qiao, W. wei, and Cui, C. wei: Reactivity and mechanism between OH and
283 phenolic pollutants: Efficiency and DFT calculation, *J Photochem Photobiol A Chem*, 407, 113025,
284 <https://doi.org/10.1016/J.JPHOTOCHEM.2020.113025>, 2021.
- 285 Cappiello, A., De Simoni, E., Fiorucci, C., Mangani, F., Palma, P., Trufelli, H., Decesari, S., Facchini, M. C., and
286 Fuzzi, S.: Molecular characterization of the water-soluble organic compounds in fogwater by ESIMS/MS,
287 *Environ Sci Technol*, 37, 1229–1240, <https://doi.org/10.1021/ES0259990>, 2003.
- 288 Chen, J., Wu, Z. J., Zhao, X., Wang, Y. J., Chen, J. C., Qiu, Y. T., Zong, T. M., Chen, H. X., Wang, B. B., Lin, P.,
289 Liu, W., Guo, S., Yao, M. S., Zeng, L. M., Wex, H., Liu, X., Hu, M., and Li, S. M.: Atmospheric Humic-Like
290 Substances (HULIS) Act as Ice Active Entities, *Geophys Res Lett*, 48, e2021GL092443,



- 291 <https://doi.org/10.1029/2021GL092443>, 2021.
- 292 Chen, S., Guo, Z., Guo, Z., Guo, Q., Zhang, Y., Zhu, B., and Zhang, H.: Sulfur isotopic fractionation and its
293 implication: Sulfate formation in PM_{2.5} and coal combustion under different conditions, *Atmos Res*, 194, 142–
294 149, <https://doi.org/10.1016/J.ATMOSRES.2017.04.034>, 2017.
- 295 Cheng, Y., He, K. B., Zheng, M., Duan, F. K., Du, Z. Y., Ma, Y. L., Tan, J. H., Yang, F. M., Liu, J. M., Zhang, X.
296 L., Weber, R. J., Bergin, M. H., and Russell, A. G.: Mass absorption efficiency of elemental carbon and water-
297 soluble organic carbon in Beijing, China, *Atmos Chem Phys*, 11, 11497–11510, [https://doi.org/10.5194/ACP-](https://doi.org/10.5194/ACP-11-11497-2011)
298 11-11497-2011, 2011.
- 299 Chung, C. E., Ramanathan, V., and Decremier, D.: Observationally constrained estimates of carbonaceous aerosol
300 radiative forcing, *Proc Natl Acad Sci U S A*, 109, 11624–11629, <https://doi.org/10.1073/PNAS.1203707109>,
301 2012.
- 302 Domingo, L. R., Seif, A., Mazarei, E., Zahedi, E., and Ahmadi, T. S.: Quasi-RRHO approximation and DFT
303 study for understanding the mechanism and kinetics of nitration reaction of benzonitrile with nitronium ion,
304 *Comput Theor Chem*, 1199, 113209, <https://doi.org/10.1016/J.COMPTC.2021.113209>, 2021.
- 305 Dong, D., Qiu, T., Du, S., Gu, Y., Li, A., Hua, X., Ning, Y., and Liang, D.: The chemical characterization and
306 source apportionment of PM_{2.5} and PM₁₀ in a typical city of Northeast China, *Urban Clim*, 47, 101373,
307 <https://doi.org/10.1016/J.UCLIM.2022.101373>, 2023.
- 308 Dou, J., Lin, P., Kuang, B. Y., and Yu, J. Z.: Reactive oxygen species production mediated by humic-like
309 substances in atmospheric aerosols: Enhancement effects by pyridine, imidazole, and their derivatives, *Environ*
310 *Sci Technol*, 49, 6457–6465, <https://doi.org/10.1021/ES5059378>, 2015.
- 311 Dutton, S. J., Williams, D. E., Garcia, J. K., Vedal, S., and Hannigan, M. P.: PM_{2.5} characterization for time
312 series studies: Organic molecular marker speciation methods and observations from daily measurements in
313 Denver, *Atmos Environ*, 43, 2018–2030, <https://doi.org/10.1016/J.ATMOSENV.2009.01.003>, 2009.
- 314 Emmenegger, C., Reinhardt, A., Hueglin, C., Zenobi, R., and Kalberer, M.: Evaporative light scattering: A novel
315 detection method for the quantitative analysis of humic-like substances in aerosols, *Environ Sci Technol*, 41,
316 2473–2478, <https://doi.org/10.1021/ES061095T>, 2007.
- 317 Finewax, Z., De Gouw, J. A., and Ziemann, P. J.: Identification and Quantification of 4-Nitrocatechol Formed
318 from OH and NO₃ Radical-Initiated Reactions of Catechol in Air in the Presence of NO_x: Implications for
319 Secondary Organic Aerosol Formation from Biomass Burning, *Environ Sci Technol*, 52, 1981–1989,
320 <https://doi.org/10.1021/ACS.EST.7B05864>, 2018.
- 321 Fountoukis, C. and Nenes, A.: ISORROPIAII: A computationally efficient thermodynamic equilibrium model
322 for K⁺-Ca²⁺-Mg²⁺-NH₄⁺-Na⁺-SO₄²⁻-NO₃⁻-Cl⁻-H₂O aerosols, *Atmos Chem Phys*, 7, 4639–4659,
323 <https://doi.org/10.5194/ACP-7-4639-2007>, 2007.
- 324 Friman, M., Aurela, M., Saarnio, K., Teinilä, K., Kesti, J., Harni, S. D., Saarikoski, S., Hyvärinen, A., and
325 Timonen, H.: Long-term characterization of organic and elemental carbon at three different background areas in
326 northern Europe, *Atmos Environ*, 310, 119953, <https://doi.org/10.1016/J.ATMOSENV.2023.119953>, 2023.
- 327 Gatzsche, K., Iinuma, Y., Tilgner, A., Mutzel, A., Berndt, T., and Wolke, R.: Kinetic modeling studies of SOA
328 formation from α -pinene ozonolysis, *Atmos Chem Phys*, 17, 13187–13211, [https://doi.org/10.5194/ACP-17-](https://doi.org/10.5194/ACP-17-13187-2017)
329 13187-2017, 2017.
- 330 Gregson, F. K. A., Gerrebos, N. G. A., Schervish, M., Nikkho, S., Schnitzler, E. G., Schwartz, C., Carlsten, C.,
331 Abbatt, J. P. D., Kamal, S., Shiraiwa, M., and Bertram, A. K.: Phase Behavior and Viscosity in Biomass Burning



- 332 Organic Aerosol and Climatic Impacts, *Environ Sci Technol*, 57, 14548–14557,
333 <https://doi.org/10.1021/ACS.EST.3C03231>, 2023.
- 334 Hatch, L. E., Luo, W., Pankow, J. F., Yokelson, R. J., Stockwell, C. E., and Barsanti, K. C.: Identification and
335 quantification of gaseous organic compounds emitted from biomass burning using two-dimensional gas
336 chromatography-time-of-flight mass spectrometry, *Atmos Chem Phys*, 15, 1865–1899,
337 <https://doi.org/10.5194/ACP-15-1865-2015>, 2015.
- 338 He, J., Zielinska, B., and Balasubramanian, R.: Composition of semi-volatile organic compounds in the urban
339 atmosphere of Singapore: Influence of biomass burning, *Atmos Chem Phys*, 10, 11401–11413,
340 <https://doi.org/10.5194/ACP-10-11401-2010>, 2010.
- 341 Hems, R. F. and Abbatt, J. P. D.: Aqueous Phase Photo-oxidation of Brown Carbon Nitrophenols: Reaction
342 Kinetics, Mechanism, and Evolution of Light Absorption, *ACS Earth Space Chem*, 2, 225–234,
343 <https://doi.org/10.1021/ACSEARTHSPACECHEM.7B00123>, 2018.
- 344 Hoffer, A., Gelencsér, A., Guyon, P., Kiss, G., Schmid, O., Frank, G. P., Artaxo, P., and Andreae, M. O.: Optical
345 properties of humic-like substances (HULIS) in biomass-burning aerosols, *Atmos Chem Phys*, 6, 3563–3570,
346 <https://doi.org/10.5194/ACP-6-3563-2006>, 2006.
- 347 Huang, L., Wang, J., Jiang, H., Chen, L., and Chen, H.: On-line determination of selenium compounds in tea
348 infusion by extractive electrospray ionization mass spectrometry combined with a heating reaction device,
349 *Chinese Chemical Letters*, 36, 109896, <https://doi.org/10.1016/J.CCLET.2024.109896>, 2025.
- 350 Huang, R. J., Yang, L., Cao, J., Chen, Y., Chen, Q., Li, Y., Duan, J., Zhu, C., Dai, W., Wang, K., Lin, C., Ni, H.,
351 Corbin, J. C., Wu, Y., Zhang, R., Tie, X., Hoffmann, T., O'Dowd, C., and Dusek, U.: Brown Carbon Aerosol in
352 Urban Xi'an, Northwest China: The Composition and Light Absorption Properties, *Environ Sci Technol*, 52,
353 6825–6833, <https://doi.org/10.1021/ACS.EST.8B02386>, 2018.
- 354 Huang, R. J., Yang, L., Shen, J., Yuan, W., Gong, Y., Guo, J., Cao, W., Duan, J., Ni, H., Zhu, C., Dai, W., Li, Y.,
355 Chen, Y., Chen, Q., Wu, Y., Zhang, R., Dusek, U., O'Dowd, C., and Hoffmann, T.: Water-Insoluble Organics
356 Dominate Brown Carbon in Wintertime Urban Aerosol of China: Chemical Characteristics and Optical
357 Properties, *Environ Sci Technol*, 54, 7836–7847, <https://doi.org/10.1021/acs.est.0c01149>, 2020.
- 358 Huang, S., Yang, X., Xu, H., Zeng, Y., Li, D., Sun, J., Ho, S. S. H., Zhang, Y., Cao, J., and Shen, Z.: Insights into
359 the nitroaromatic compounds, formation, and light absorption contributing emissions from various geological
360 maturity coals, *Science of The Total Environment*, 870, 162033,
361 <https://doi.org/10.1016/J.SCITOTENV.2023.162033>, 2023.
- 362 Huo, Y., Guo, Z., Li, Q., Wu, D., Ding, X., Liu, A., Huang, D., Qiu, G., Wu, M., Zhao, Z., Sun, H., Song, W., Li,
363 X., Chen, Y., Wu, T., and Chen, J.: Chemical Fingerprinting of HULIS in Particulate Matters Emitted from
364 Residential Coal and Biomass Combustion, *Environ Sci Technol*, 55, 3593–3603,
365 <https://doi.org/10.1021/acs.est.0c08518>, 2021.
- 366 Jiang, H., Cai, J., Feng, X., Chen, Y., Wang, L., Jiang, B., Liao, Y., Li, J., Zhang, G., Mu, Y., and Chen, J.:
367 Aqueous-Phase Reactions of Anthropogenic Emissions Lead to the High Chemodiversity of Atmospheric
368 Nitrogen-Containing Compounds during the Haze Event, *Environ Sci Technol*, 57, 16500–16511,
369 <https://doi.org/10.1021/ACS.EST.3C06648>, 2023.
- 370 Krivácsy, Z., Kiss, G., Varga, B., Galambos, I., Sárvári, Z., Gelencsér, A., Molnár, Á., Fuzzi, S., Facchini, M. C.,
371 Zappoli, S., Andracchio, A., Alsberg, T., Hansson, H. C., and Persson, L.: Study of humic-like substances in fog
372 and interstitial aerosol by size-exclusion chromatography and capillary electrophoresis, *Atmos Environ*, 34,



- 373 4273–4281, [https://doi.org/10.1016/S1352-2310\(00\)00211-9](https://doi.org/10.1016/S1352-2310(00)00211-9), 2000.
- 374 Kroflič, A., Anders, J., Drventić, I., Mettke, P., Böge, O., Mutzel, A., Kleffmann, J., and Herrmann, H.: Guaiacol
- 375 Nitration in a Simulated Atmospheric Aerosol with an Emphasis on Atmospheric Nitrophenol Formation
- 376 Mechanisms, *ACS Earth Space Chem*, 5, 1083–1093,
- 377 <https://doi.org/10.1021/ACSEARTHSPACECHEM.1C00014>, 2021.
- 378 Laskin, A., Laskin, J., and Nizkorodov, S. A.: Chemistry of Atmospheric Brown Carbon, *Chem Rev*, 115, 4335–
- 379 4382, <https://doi.org/10.1021/CR5006167>, 2015.
- 380 Li, Y. and Shiraiwa, M.: Timescales of secondary organic aerosols to reach equilibrium at various temperatures
- 381 and relative humidities, *Atmos Chem Phys*, 19, 5959–5971, <https://doi.org/10.5194/ACP-19-5959-2019>, 2019.
- 382 Li, Y., A. Day, D., Stark, H., L. Jimenez, J., and Shiraiwa, M.: Predictions of the glass transition temperature and
- 383 viscosity of organic aerosols from volatility distributions, *Atmos Chem Phys*, 20, 8103–8122,
- 384 <https://doi.org/10.5194/ACP-20-8103-2020>, 2020.
- 385 Liang, L., Engling, G., Liu, C., Xu, W., Liu, X., Cheng, Y., Du, Z., Zhang, G., Sun, J., and Zhang, X.: Measurement report: Chemical characteristics of PM_{2.5} during typical biomass burning season at an agricultural
- 386 site of the North China Plain, *Atmos Chem Phys*, 21, 3181–3192, <https://doi.org/10.5194/ACP-21-3181-2021>,
- 387 2021.
- 388
- 389 Limbeck, A., Handler, M., Neuberger, B., Klatzer, B., and Puxbaum, H.: Carbon-specific analysis of humic-like
- 390 substances in atmospheric aerosol and precipitation samples, *Anal Chem*, 77, 7288–7293,
- 391 <https://doi.org/10.1021/AC050953L>, 2005.
- 392 Lin, P., Rincon, A. G., Kalberer, M., and Yu, J. Z.: Elemental composition of HULIS in the Pearl River Delta
- 393 Region, China: Results inferred from positive and negative electrospray high resolution mass spectrometric data,
- 394 *Environ Sci Technol*, 46, 7454–7462, <https://doi.org/10.1021/es300285d>, 2012.
- 395 Lin, P., Bluvshstein, N., Rudich, Y., Nizkorodov, S. A., Laskin, J., and Laskin, A.: Molecular Chemistry of
- 396 Atmospheric Brown Carbon Inferred from a Nationwide Biomass Burning Event, *Environ Sci Technol*, 51,
- 397 11561–11570, <https://doi.org/10.1021/ACS.EST.7B02276>, 2017.
- 398 Liu, W., Liao, K., Chen, Q., He, L., Liu, Y., and Kuwata, M.: Existence of Crystalline Ammonium Sulfate Nuclei
- 399 Affects Chemical Reactivity of Oleic Acid Particles Through Heterogeneous Nucleation, *Journal of Geophysical*
- 400 *Research: Atmospheres*, 128, e2023JD038675, <https://doi.org/10.1029/2023JD038675>, 2023.
- 401 Lu, S., Win, M. S., Zeng, J., Yao, C., Zhao, M., Xiu, G., Lin, Y., Xie, T., Dai, Y., Rao, L., Zhang, L., Yonemochi,
- 402 S., and Wang, Q.: A characterization of HULIS-C and the oxidative potential of HULIS and HULIS-Fe(II)
- 403 mixture in PM_{2.5} during hazy and non-hazy days in Shanghai, *Atmos Environ*, 219, 117058,
- 404 <https://doi.org/10.1016/J.ATMOSENV.2019.117058>, 2019.
- 405 Ma, G., Liu, X., Wang, J., Li, M., Dong, Z., Li, X., Wang, L., Han, Y., and Cao, J.: Characteristics and health
- 406 risk assessment of indoor and outdoor PM_{2.5} in a rural village, in Northeast of China: impact of coal and biomass
- 407 burning, *Environ Geochem Health*, 45, 9639–9652, <https://doi.org/10.1007/S10653-023-01755-W>, 2023.
- 408 Ma, Y., Cheng, Y., Qiu, X., Cao, G., Kuang, B., Yu, J. Z., and Hu, D.: Optical properties, source apportionment
- 409 and redox activity of humic-like substances (HULIS) in airborne fine particulates in Hong Kong, *Environmental*
- 410 *Pollution*, 255, 113087, <https://doi.org/10.1016/J.ENVPOL.2019.113087>, 2019.
- 411 Mayorga, R. J., Zhao, Z., and Zhang, H.: Formation of secondary organic aerosol from nitrate radical oxidation
- 412 of phenolic VOCs: Implications for nitration mechanisms and brown carbon formation, *Atmos Environ*, 244,
- 413 117910, <https://doi.org/10.1016/J.ATMOSENV.2020.117910>, 2021.



- 414 Mikhailov, E., Vlasenko, S., Martin, S. T., Koop, T., and Pöschl, U.: Amorphous and crystalline aerosol particles
415 interacting with water vapor: Conceptual framework and experimental evidence for restructuring, phase
416 transitions and kinetic limitations, *Atmos Chem Phys*, 9, 9491–9522, <https://doi.org/10.5194/ACP-9-9491-2009>,
417 2009.
- 418 Nenes, A., Pandis, S. N., and Pilinis, C.: ISORROPIA: A new thermodynamic equilibrium model for multiphase
419 multicomponent inorganic aerosols, *Aquat Geochem*, 4, 123–152, <https://doi.org/10.1023/A:1009604003981>,
420 1998.
- 421 Pratt, K. A., Fiddler, M. N., Shepson, P. B., Carlton, A. G., and Surratt, J. D.: Organosulfates in cloud water
422 above the Ozarks’ isoprene source region, *Atmos Environ*, 77, 231–238,
423 <https://doi.org/10.1016/J.ATMOENV.2013.05.011>, 2013.
- 424 Qiu, Y., Qiu, T., Wu, Z., Liu, Y., Fang, W., Man, R., Liu, Y., Wang, J., Meng, X., Chen, J., Liang, D., Guo, S.,
425 and Hu, M.: Observational Evidence of Brown Carbon Photobleaching in Urban Atmosphere at Molecular Level,
426 *Environ Sci Technol Lett*, <https://doi.org/10.1021/ACS.ESTLETT.4C00647>, 2024.
- 427 Roelofs, G. J.: A steady-state analysis of the temperature responses of water vapor and aerosol lifetimes, *Atmos*
428 *Chem Phys*, 13, 8245–8254, <https://doi.org/10.5194/ACP-13-8245-2013>, 2013.
- 429 Schervish, M. and Donahue, N. M.: Peroxy radical chemistry and the volatility basis set, *Atmos Chem Phys*, 20,
430 1183–1199, <https://doi.org/10.5194/ACP-20-1183-2020>, 2020.
- 431 Schnitzler, E. G. and Abbatt, J. P. D.: Heterogeneous OH oxidation of secondary brown carbon aerosol, *Atmos*
432 *Chem Phys*, 18, 14539–14553, <https://doi.org/10.5194/ACP-18-14539-2018>, 2018.
- 433 Schnitzler, E. G., Gerrebos, N. G. A., Carter, T. S., Huang, Y., Heald, C. L., Bertram, A. K., and Abbatt, J. P. D.:
434 Rate of atmospheric brown carbon whitening governed by environmental conditions, *Proc Natl Acad Sci U S A*,
435 119, e2205610119, <https://doi.org/10.1073/PNAS.2205610119>, 2022.
- 436 Serafeim, E., Besis, A., Kouras, A., Farias, C. N., Yera, A. B., Pereira, G. M., Samara, C., and de Castro
437 Vasconcellos, P.: Oxidative potential of ambient PM_{2.5} from São Paulo, Brazil: Variations, associations with
438 chemical components and source apportionment, *Atmos Environ*, 298, 119593,
439 <https://doi.org/10.1016/J.ATMOENV.2023.119593>, 2023.
- 440 Shiraiwa, M., Ammann, M., Koop, T., and Pöschl, U.: Gas uptake and chemical aging of semisolid organic
441 aerosol particles, *Proc Natl Acad Sci U S A*, 108, 11003–11008, <https://doi.org/10.1073/PNAS.1103045108>,
442 2011.
- 443 Shiraiwa, M., Li, Y., Tsimpidi, A. P., Karydis, V. A., Berkemeier, T., Pandis, S. N., Lelieveld, J., Koop, T., and
444 Pöschl, U.: Global distribution of particle phase state in atmospheric secondary organic aerosols, *Nature*
445 *Communications* 2017 8:1, 8, 1–7, <https://doi.org/10.1038/ncomms15002>, 2017.
- 446 Slade, J. H., Shiraiwa, M., Arangio, A., Su, H., Pöschl, U., Wang, J., and Knopf, D. A.: Cloud droplet activation
447 through oxidation of organic aerosol influenced by temperature and particle phase state, *Geophys Res Lett*, 44,
448 1583–1591, <https://doi.org/10.1002/2016GL072424>, 2017.
- 449 Song, J., Li, M., Jiang, B., Wei, S., Fan, X., and Peng, P.: Molecular Characterization of Water-Soluble Humic
450 like Substances in Smoke Particles Emitted from Combustion of Biomass Materials and Coal Using Ultrahigh-
451 Resolution Electrospray Ionization Fourier Transform Ion Cyclotron Resonance Mass Spectrometry, *Environ*
452 *Sci Technol*, 52, 2575–2585, <https://doi.org/10.1021/acs.est.7b06126>, 2018.
- 453 Song, J., Li, M., Zou, C., Cao, T., Fan, X., Jiang, B., Yu, Z., Jia, W., and Peng, P.: Molecular Characterization of
454 Nitrogen-Containing Compounds in Humic-like Substances Emitted from Biomass Burning and Coal



- 455 Combustion, *Environ Sci Technol*, 56, 119–130, <https://doi.org/10.1021/acs.est.1c04451>, 2022a.
- 456 Song, L., Chingin, K., Wang, M., Zhong, D., Chen, H., and Xu, J.: Polarity-Specific Profiling of Metabolites in
457 Single Cells by Probe Electrophoresis Mass Spectrometry, *Anal Chem*, 94, 4175–4182,
458 <https://doi.org/10.1021/ACS.ANALCHEM.1C03997>, 2022b.
- 459 Song, L., Zhong, L., Li, T., Chen, Y., Zhang, X., Chingin, K., Zhang, N., Li, H., Hu, L., Guo, D., Chen, H., Su,
460 R., and Xu, J.: Chemical Fingerprinting of PM_{2.5} via Sequential Speciation Analysis Using Electrochemical
461 Mass Spectrometry, *Environ Sci Technol*, 58, <https://doi.org/10.1021/ACS.EST.4C01682>, 2024.
- 462 Souza, K. F., Carvalho, L. R. F., Allen, A. G., and Cardoso, A. A.: Diurnal and nocturnal measurements of PAH,
463 nitro-PAH, and oxy-PAH compounds in atmospheric particulate matter of a sugar cane burning region, *Atmos*
464 *Environ*, 83, 193–201, <https://doi.org/10.1016/J.ATMOENV.2013.11.007>, 2014.
- 465 Tao, Y. and Murphy, J. G.: Simple Framework to Quantify the Contributions from Different Factors Influencing
466 Aerosol pH Based on NH_xPhase-Partitioning Equilibrium, *Environ Sci Technol*, 55, 10310–10319,
467 <https://doi.org/10.1021/ACS.EST.1C03103>, 2021.
- 468 Virtanen, A., Joutsensaari, J., Koop, T., Kannosto, J., Yli-Pirilä, P., Leskinen, J., Mäkelä, J. M., Holopainen, J.
469 K., Pöschl, U., Kulmala, M., Worsnop, D. R., and Laaksonen, A.: An amorphous solid state of biogenic secondary
470 organic aerosol particles, *Nature* 2010 467:7317, 467, 824–827, <https://doi.org/10.1038/nature09455>, 2010.
- 471 Voliotis, A., Prokeš, R., Lammel, G., and Samara, C.: New insights on humic-like substances associated with
472 wintertime urban aerosols from central and southern Europe: Size-resolved chemical characterization and optical
473 properties, *Atmos Environ*, 166, 286–299, <https://doi.org/10.1016/J.ATMOENV.2017.07.024>, 2017.
- 474 Wach, P., Spólnik, G., Surratt, J. D., Blaziak, K., Rudzinski, K. J., Lin, Y. H., Maenhaut, W., Danikiewicz, W.,
475 Claeys, M., and Szmigielski, R.: Structural Characterization of Lactone-Containing MW 212 Organosulfates
476 Originating from Isoprene Oxidation in Ambient Fine Aerosol, *Environ Sci Technol*, 54, 1415–1424,
477 <https://doi.org/10.1021/ACS.EST.9B06190>, 2020.
- 478 Wang, D., Shen, Z., Zhang, Q., Lei, Y., Zhang, T., Huang, S., Sun, J., Xu, H., and Cao, J.: Winter brown carbon
479 over six of China's megacities: Light absorption, molecular characterization, and improved source
480 apportionment revealed by multilayer perceptron neural network, *Atmos Chem Phys*, 22, 14893–14904,
481 <https://doi.org/10.5194/ACP-22-14893-2022>, 2022.
- 482 Wang, H., Gao, Y., Wang, S., Wu, X., Liu, Y., Li, X., Huang, D., Lou, S., Wu, Z., Guo, S., Jing, S., Li, Y., Huang,
483 C., Tyndall, G. S., Orlando, J. J., and Zhang, X.: Atmospheric Processing of Nitrophenols and Nitrocresols From
484 Biomass Burning Emissions, *Journal of Geophysical Research: Atmospheres*, 125, e2020JD033401,
485 <https://doi.org/10.1029/2020JD033401>, 2020.
- 486 Wang, Y., Hu, M., Lin, P., Guo, Q., Wu, Z., Li, M., Zeng, L., Song, Y., Zeng, L., Wu, Y., Guo, S., Huang, X., and
487 He, L.: Molecular Characterization of Nitrogen-Containing Organic Compounds in Humic-like Substances
488 Emitted from Straw Residue Burning, *Environ Sci Technol*, 51, 5951–5961,
489 <https://doi.org/10.1021/acs.est.7b00248>, 2017a.
- 490 Wang, Y., Hu, M., Lin, P., Tan, T., Li, M., Xu, N., Zheng, J., Du, Z., Qin, Y., Wu, Y., Lu, S., Song, Y., Wu, Z.,
491 Guo, S., Zeng, L., Huang, X., and He, L.: Enhancement in Particulate Organic Nitrogen and Light Absorption
492 of Humic-Like Substances over Tibetan Plateau Due to Long-Range Transported Biomass Burning Emissions,
493 *Environ Sci Technol*, 53, 14222–14232, <https://doi.org/10.1021/acs.est.9b06152>, 2019.
- 494 Wang, Z. M., Zheng, M., Xie, Y. B., Li, X. X., Zeng, M., Cao, H. Bin, and Guo, L.: Molecular dynamics
495 simulation of ozonation of p-nitrophenol at room temperature with ReaxFF force field, *Wuli Huaxue Xuebao/*



- 496 Acta Physico - Chimica Sinica, 33, 1399–1410, <https://doi.org/10.3866/PKU.WHXB201704132>, 2017b.
- 497 Wu, Z., Wang, Y., Tan, T., Zhu, Y., Li, M., Shang, D., Wang, H., Lu, K., Guo, S., Zeng, L., and Zhang, Y.: Aerosol
- 498 Liquid Water Driven by Anthropogenic Inorganic Salts: Implying Its Key Role in Haze Formation over the North
- 499 China Plain, Environ Sci Technol Lett, 5, 160–166, <https://doi.org/10.1021/ACS.ESTLETT.8B00021>, 2018.
- 500 Xu, H., Gu, Y., Bai, Y., Li, D., Liu, M., Wang, Z., Zhang, Q., Sun, J., and Shen, Z.: Exploration and comparison
- 501 of the relationship between PAHs and ROS in PM_{2.5} emitted from multiple anthropogenic sources in the
- 502 Guanzhong Plain, China, Science of The Total Environment, 915, 170229, <https://doi.org/10.1016/J.SCITOTENV.2024.170229>, 2024.
- 503
- 504 Yuan, W., Huang, R. J., Yang, L., Ni, H., Wang, T., Cao, W., Duan, J., Guo, J., Huang, H., and Hoffmann, T.:
- 505 Concentrations, optical properties and sources of humic-like substances (HULIS) in fine particulate matter in
- 506 Xi'an, Northwest China, Science of the Total Environment, 789, <https://doi.org/10.1016/j.scitotenv.2021.147902>,
- 507 2021.
- 508 Zhao, T., Yang, L., Huang, Q., Zhang, Y., Bie, S., Li, J., Zhang, W., Duan, S., Gao, H., and Wang, W.: PM_{2.5}-
- 509 bound polycyclic aromatic hydrocarbons (PAHs) and their derivatives (nitrated-PAHs and oxygenated-PAHs) in
- 510 a road tunnel located in Qingdao, China: Characteristics, sources and emission factors, Science of The Total
- 511 Environment, 720, 137521, <https://doi.org/10.1016/J.SCITOTENV.2020.137521>, 2020.
- 512 Zou, C., Li, M., Cao, T., Zhu, M., Fan, X., Peng, S., Song, J., Jiang, B., Jia, W., Yu, C., Song, H., Yu, Z., Li, J.,
- 513 Zhang, G., and Peng, P.: Comparison of solid phase extraction methods for the measurement of humic-like
- 514 substances (HULIS) in atmospheric particles, Atmos Environ, 225, 117370, <https://doi.org/10.1016/J.ATMOSENV.2020.117370>, 2020.
- 515
- 516 Zou, C., Cao, T., Li, M., Song, J., Jiang, B., Jia, W., Li, J., Ding, X., Yu, Z., Zhang, G., and Peng, P.: Measurement
- 517 report: Changes in light absorption and molecular composition of water-soluble humic-like substances during a
- 518 winter haze bloom-decay process in Guangzhou, China, Atmos Chem Phys, 23, 963–979, <https://doi.org/10.5194/ACP-23-963-2023>, 2023.
- 519